Phase Coherent Timing of RX J0806.3+1527 with ROSAT and CHANDRA

Tod E. Strohmayer

Laboratory for High Energy Astrophysics, NASA's Goddard Space Flight Center, Greenbelt, MD 20771; stroh@clarence.gsfc.nasa.gov

ABSTRACT

RX J0806.3+1527 is an ultra-compact, double degenerate binary with the shortest known orbital period (321.5 s). Hakala et al. (2003) have recently reported new optical measurements of the orbital frequency of the source which indicate that the frequency has increased over the ≈ 9 years since the earliest ROSAT observations. They find two candidate solutions for the long term change in the frequency; $\dot{\nu} \approx 3$ or 6×10^{-16} Hz s^{-1}. Here we present the results of a phase coherent timing study of the archival ROSAT and Chandra data for RX J0806.3+1527 in the light of these new constraints. We find that the ROSAT – Chandra timing data are consistent with both of the solutions reported by Hakala et al., but that the higher $\dot{\nu} = 6.1 \times 10^{-16}$ Hz s^{-1} solution is favored at the $\approx 97\%$ level. This large a $\dot{\nu}$ can be accomodated by an $\approx 1 M_{\odot}$ detached double degenerate system powered in the X-ray by electrical energy (Wu et al. 2002). With such a large $\dot{\nu}$ the system provides a unique opportunity to explore the interaction of gravitational radiation and electromagnetic torques on the evolution of an ultracompact binary.

Subject headings: Binaries: close - Stars: individual (RX J0806.3+1527, RX J1914.4+2456) - Stars: white dwarfs – X-rays: binaries – Gravitational Waves

1. Introduction

Double degenerate systems containing a pair of interacting white dwarfs are the most compact binaries known. Evidence has been mounting recently that the two systems with the shortest inferred orbital periods, RX J1914.4+2456 (569 s, hereafter J1914) and RX J0806.3+1527 (321 s, hereafter J0806), may represent a new class of double degenerates whose X-ray flux is powered by a unipolar induction process rather than accretion (see Wu et al. 2002; Strohmayer 2002; and Hakala et al. 2003). These objects have much in common

(see Cropper et al. 2003 for a recent review). Their X-ray lightcurves show 100% modulation with a sharp rise and more gradual decay, suggestive of a small X-ray emitting region on the primary (Cropper et al. 1998). In both systems the optical maximum lags the X-ray maximum by about 0.6 of a cycle, consistent with the optical variations resulting from X-ray heating of the secondary (Ramsay et al. 2000; Israel et al. 2003).

Of the models that have been proposed for J1914 and J0806, the Intermediate Polar (IP) scenario is looking increasingly unlikely (see Cropper et al. 2003 for a discussion). All the remaining models are variants of a double degenerate scenario. In the Polar model the primary is magnetic, the binary is synchronized and the X-ray flux is accretion driven (Cropper et al. 1998). Some difficulties with this model are the lack of circular polarization in the optical (although magnetic fields weak enough to preclude detection of polarization may still be able to enforce synchronization), and the lack of any hard (> 2 keV) spectral component, as is usually seen in Polars. Another variant is the direct accretor model (Marsh & Steeghs 2002; Ramsay et al. 2002). In this model both components are non-magnetic, and the accretion stream impacts directly onto the surface of the primary (i.e. without the formation of an accretion disk). Shortcomings of this model include the stable X-ray to optical phasing of the lightcurves, and the need for a relatively low mass ($< 0.5 M_{\odot}$) primary.

An important constraint on the models can be obtained by measuring the orbital evolution in these systems. If the donors are degenerate, then stable accretion will lead to a widening of the orbit and a decrease in the orbital frequency, $\dot{\nu}$. From a timing study of archival ROSAT and ASCA data Strohmayer (2002) found evidence that the orbital frequency of J1914 is increasing at a rate consistent with loss of orbital angular momentum to gravitational radiation. Recently, Hakala et al. (2003) have used archival ROSAT and new optical timing measurements of J0806 to constrain the orbital evolution. They find that, similarly to J1914, the orbital frequency of J0806 is also increasing, but at a rate that is factor of about 30 or more higher than for J1914. Considering the more compact orbit in J0806, and the strong $\nu^{11/3}$ orbital frequency dependence of gravitational radiation, a substantially higher $\dot{\nu}$ is not unexpected.

Hakala et al. (2003) used period measurements from ROSAT in 1994 - 1995 as well as more recent optical data from the ESO VLT and the Nordic Optical Telescope (NOT) on La Palma to explore the orbital evolution of J0806. They derived a frequency history at three epochs and deduced a frequency increase. Here we report the results of a coherent, phase timing study of J0806 using the 1994 - 1995 ROSAT data combined with the public Chandra observations from November, 2001. Hakala et al. (2003) did not use the Chandra data in their study because it is too short in duration for a precision frequency measurement. By themselves the ROSAT and Chandra data are insufficient to unambiguously constrain

the frequency evolution because of their sparseness. However, in the light of the additional constraints on $\dot{\nu}$ provided by the Hakala et al. study, we can use phase timing analysis of the ROSAT and Chandra data to test for consistency with and to see if the data favor one of the possible solutions found by Hakala et al. (2003). We find that the ROSAT and Chandra phase timing data are consistent with the two possible $\dot{\nu}$ solutions found by Hakala et al. (2003), and that the solution with the larger $\dot{\nu} \approx 6 \times 10^{-16}$ Hz s^{-1} provides a better fit to the phase timing data and is preferred at about the 97% confidence level. We also briefly discuss the implications of this finding for the models for J0806 and its cousin source J1914.

2. Data Extraction and Analysis

The ROSAT HRI observed J0806 for a total of ≈ 16 ksec in the interval from October, 1994 through April, 1995. Burwitz & Reinsch (2001) reported on the pulse timing from these observations. Chandra observed J0806 for 20 ksec in November, 2001. Spectroscopy from this observation is reported by Israel et al. (2003). All these data are now in the public domain. We used standard HEASARC FTOOLS data analysis packages (i.e., XSELECT) to extract and analyse the data. We began by producing images and extracting source events. We next applied barycentric corrections to the event times for each observation. We used the standard mission FTOOLS in conjunction with the ROSAT and Chandra orbital and JPL (DE200) solar system ephemerides (Standish et al. 1992). For the source position we used the coordinates, ($\alpha = 08^h06^m23.2^s$, $\delta = 15°27'30.2''$:J2000), obtained by Israel et al. (2002) from their study of the optical-infrared counterpart to J0806. Our analysis resulted in a total of 725 and 6076 photons from the ROSAT and Chandra observations, respectively.

2.1. Coherent Timing Methods

We performed our coherent timing studies using the Z_n^2 statistic (Buccheri 1983; see also Strohmayer 2002 and Strohmayer & Markwardt 2002 for examples of the use of this statistic in a similar context). We use a two parameter phase model, with $\phi(t) = \nu_0(t-t_0)+\frac{1}{2}\dot{\nu}(t-t_0)^2$. Since the methods are described elsewhere we do not repeat the details here. From their study of the ROSAT data, Burwitz & Reinsch (2001) found two candidate periods, 321.5393 or 321.5465 s, with an uncertainty of 0.4 ms. We began by first analyzing just the ROSAT events and confirm these results. In terms of frequencies they are 3.1100392 and 3.10997285 mHz, respectively, with an uncertainty of about 4 nHz.

From their analysis of the orbital frequency at three different epochs spanning about 9.2

years Hakala et al. (2003) found two possible solutions for $\dot{\nu}$. Two solutions were possible because of the ambiguity in the period obtained from the ROSAT observations. We used the ROSAT and Chandra data to perform a grid search in the $\nu - \dot{\nu}$ plane in the vicinity of these two possible solutions in order to determine whether the combined ROSAT – Chandra data are consistent with them and to see if perhaps one of them is favored. We calculated a χ^2 statistic by comparing the model predicted phases with the observed phases (see Strohmayer 2002 for details). We had a total of 31 phase measurements, 10 from the ROSAT epoch and 21 from the Chandra data, giving us fits with 29 degrees of freedom. The results of our grid search are summarized in Figure 1. Panel (a) shows the 1σ confidence contours in the vicinity of $\dot{\nu} = 3.1 \times 10^{-16}$ Hz s^{-1}, while panel (b) shows the same quantities in the vicinity of the larger $\dot{\nu}$ solution, $\dot{\nu} = 6.1 \times 10^{-16}$ Hz s^{-1}. In each figure the best solution and errors from the Hakala et al. study are marked by the solid and dashed horizontal lines, respectively. We find that the ROSAT – Chandra timing data have solutions which are consistent with both of the Hakala et al. (2003) solutions. However, we also find that the $\dot{\nu} = 6.11 \times 10^{-16}$ Hz s^{-1} gives a better fit. This solution has a minimum $\chi^2 = 33.1$, while the other $\dot{\nu}$ solution has a minimum $\chi^2 = 40.8$. The $\Delta\chi^2 = 7.7$ between the two solutions favors the higher $\dot{\nu}$ solution at about the 97% level. Although this level of significance does not provide concrete proof, it is suggestive that the higher $\dot{\nu}$ solution is the correct one.

Figures 2a and 2b compare the phase residuals computed from the models with $\dot{\nu} = 3.1 \times 10^{-16}$ and 6.1×10^{-16} Hz s^{-1}, respectively. Interestingly, much of the improvement in the fit results from the improvement of the residuals to the ROSAT data. Although this may at first seem surprising, these data span an interval of about 7 months. A $\dot{\nu}$ of 6×10^{-16} Hz s^{-1} produces a phase advance on the order of ≈ 0.2 cycles over such a time span, so that the ROSAT data are in principle sensitive to a $\dot{\nu}$ of this size. We note that without the *a priori* constraints on $\dot{\nu}$ provided by the Hakala et al. results, the ROSAT – Chandra data can be fit by a number of different combinations of ν and $\dot{\nu}$. Some of these "alias" solutions can be seen in Figure 1a and b.

2.2. Discussion and Implications

The observations by Hakala et al. (2003) of the orbital frequency history of J0806 provide strong evidence that the orbit is decaying at a rate as predicted by the ultra-compact binary model in which the loss of orbital angular momentum is dominated by gravitational radiation and there is no mass exchange between the two stars. We have shown that phase coherent timing of the ROSAT and Chandra data are consistent with the rate of orbital frequency increase deduced by Hakala et al (2003), and that the ROSAT - Chandra data

provide suggestive evidence that the higher $\dot{\nu}$ value is the correct one.

For a detached binary with a circular orbit the rate of change of the orbital frequency due to gravitational radiation is (see for example, Evans, Iben & Smarr 1987; Taylor & Weisberg 1989)

$$\dot{\nu}_{gr} = 1.64 \times 10^{-17} \left(\frac{\nu}{10^{-3}\ \mathrm{Hz}}\right)^{5} \left(\frac{\mu}{M_{\odot}}\right) \left(\frac{a}{10^{10}\ \mathrm{cm}}\right)^{2} \ \mathrm{Hz\ s^{-1}}\ , \tag{1}$$

where, ν, μ, and a are the orbital frequency, reduced mass and orbital separation of the components, respectively. If the orbital decay results only from gravitational radiation losses and there is no mass transfer, then the constraint on $\dot{\nu}$ implies a constraint on the so called "chirp mass,"

$$\left(\frac{M_{ch}}{M_{\odot}}\right)^{5/3} = \left(\frac{\mu}{M_{\odot}}\right) \left(\frac{m_1 + m_2}{M_{\odot}}\right)^{2/3} = 2.7 \times 10^{16} \left(\frac{\nu}{10^{-3}\ \mathrm{Hz}}\right)^{-11/3} \dot{\nu}\ . \tag{2}$$

This constraint follows directly from equation (1) and the use of Kepler's law to substitute for the orbital separation, a. This expression also assumes no spin - orbit coupling. If the stars remain synchronized with the orbit, then the expression is modified to account for the angular momentum required to spin up the components as the orbit shrinks. We can use these expressions to constrain the component masses of J0806 under the assumption that the orbital dissipation is dominated by gravitational radiation. Figure 3 shows the 1σ contours in the mass plane for the two possible $\dot{\nu}$ solutions. Contours calculated assuming no spin - orbit coupling (solid curves), and full synchronization (dashed curves) are also shown. The dotted lines mark the region where the mass ratio, $q = m_{sec}/m_{prim}$ is between 0.5 and 1. Binary evolution calculations for ultra-compact, double degenerate systems suggest that they preferrentially form with mass ratios ~ 1 (see Nelemans et al. 2001, Napiwotzki et al. 2002). The inferred masses are consistent with double degenerate system with a total system mass $\sim 1 M_{\odot}$ (see also Hakala et al. 2003).

The inferred rate of orbital evolution in J0806 is so large that it opens up a unique opportunity for phase timing observations to track its evolution in detail. For example, at a rate of 6×10^{-16} Hz s^{-1} the phase will advance by ≈ 0.3 cycles in only a year. A glance at Figure 2 confirms that such changes can be easily measured with Chandra in less than a year.

The inferred spin-up of the system is difficult to understand in the context of an accreting double-degenerate system. Stable accretion requires that the orbital separation increases, contrary to the observations. (see for example, Rappaport, Joss & Webbink 1982; Nelemans et al. 2001). As noted by Strohmayer (2002) and Hakala et al. (2003), the observation of spin-up in J1914 and J0806 can be accomodated in the unipolar induction, or electric

star model of Wu et al. (2002). Indeed, for the large $\dot{\nu}$ inferred from J0806, it is possible that a majority of the orbital dissipation may arise from the electromagnetic torques. It is likely that instabilities in this process as, for example, caused by induced magnetic fields, will introduce variability both in the X-ray flux and the electromagnetic torque (Cropper et al. 2003). With precise, phase coherent timing, it is possible that such variations could be detected, and the electric star model explored in detail. As noted by Hakala et al. (2003), this would also be possible with independent optically derived constraints on the component masses, and would also be facilitated by future gravitational wave measurements (with, for example LISA).

References

Buccheri, R. et al. 1983, A&A, 128, 245

Burwitz, V. & Reinsch, K. 2001, X-ray Astronomy: stellar endpoints, AGN, and the diffuse X-ray background, Bologna, Italy, eds. White, N. E., Malaguti, G., and Palumbo, G., AIP conference proceedings, 599, 522.

Cropper, M., Ramsay, G., Wu, K. & Hakala, P. 2003, in Proc. Third Workshop on Magnetic CVs, Cape Town, (astro-ph/0302240).

Cropper, M. et al. 1998, MNRAS, 293, L57.

Evans, C. R., Iben, I. & Smarr, L. 1987, ApJ, 323, 129.

Hakala, P. et al. 2003, MNRAS, in press (astro-ph/0305283).

Iben, I. & Tutukov, A. V. 1991, ApJ, 370, 615.

Israel, G. L. et al. 2003, in Proc. Third Workshop on Magnetic CVs, Cape Town, (astro-ph/0303124).

Israel, G. L. et al. 2002, A&A, 386, L131.

Israel, G. L. et al. 1999, A&A, 349, L1.

Marsh, T. R. & Steeghs, D. 2002, MNRAS, 331, L7.

Motch, C. et al. 1996, A&A, 307, 459.

Napiwotzki, R. et al. 2002, A&A, 386, 957.

Nelemans, G., Portegies Zwart, S. F., Verbunt, F. & Yungelson, L. R. 2001a, A&A, 368, 939.

Ramsay, G., Cropper, M., Wu, K., Mason, K. O., & Hakala, P. 2000, MNRAS, 311, 75.

Ramsay, G., et al. 2002, MNRAS, 333, 575.

Rappaport, S., Joss, P. C. & Webbink, R. F. 1982, ApJ, 254, 616.

Standish, E. M., Newhall, X. X., Williams, J. G. & Yeomans, D. K 1992, in Explanatory Supplememt to the Astronomical Almanac, ed. P. K. Seidelmann (Mill Valley: University Science), 239.

Strohmayer, T. E. 2002, ApJ, 581, 577.

Strohmayer, T. E., & Markwardt, C. B., 2002, ApJ, 577, 337.

Strohmayer, T. E., & Markwardt, C. B., 1999, ApJ, 516, L81.

Taylor, J. H. & Weisberg, J. M. 1989, ApJ, 345, 434.

Wu, K., Cropper, M., Ramsay, G. & Sekiguchi, K. 2002, MNRAS, 331, 221.

Figure Captions

Fig. 1.— Results of our ROSAT – Chandra timing study for J0806. (a) The 1σ confidence contours in the ν, $\dot{\nu}$ plane are shown in the vicinity of the lower $\dot{\nu} \approx 3 \times 10^{-16}$ Hz s^{-1} solution of Hakala et al. (2003). The best χ^2 for this solution was $\chi^2_{min} = 40.8$. The Hakala et al. solution and 1σ errors are marked by the horizontal solid and dashed lines, respectively. The nearby, "alias" solutions result from the sparseness of the ROSAT and Chandra observations. (b) Same as for Figure 1a, but in the vicinity of the $\dot{\nu} = 6 \times 10^{-16}$ Hz s^{-1} solution of Hakala et al. (2003). This solution has a better fit with $\chi^2_{min} = 33.1$.

Fig. 2.— Phase residuals from our ROSAT – Chandra timing study for J0806. (a) The phase residuals from the best fit consistent with the $\dot{\nu} \approx 3 \times 10^{-16}$ Hz s^{-1} solution of Hakala et al. (2003) are shown. The individual phase measurements are on the x-axis, and the vertical dotted line denotes the ROSAT and Chandra epochs. The long time gaps are essentially removed in this representation. (b) Same as Figure 2a, but for the $\dot{\nu} \approx 6 \times 10^{-16}$ Hz s^{-1} solution of Hakala et al. (2003). This solution has the better overall χ^2. Most of the improvement comes from the better fit to the ROSAT phases.

Fig. 3.— Constraints on the component masses of J0806 assuming that the orbital decay results only from gravitational radiation losses. The 1σ constraints for the 6×10^{-16} Hz s^{-1} (upper) and 3×10^{-16} Hz s^{-1} (lower) are shown. In each case the solid and dashed curves are derived assuming no spin - orbit coupling, and full synchronization, respectively. The region between the dotted lines marks the phase space for which $0.5 < q = m_{sec}/m_{prim} < 1.0$.

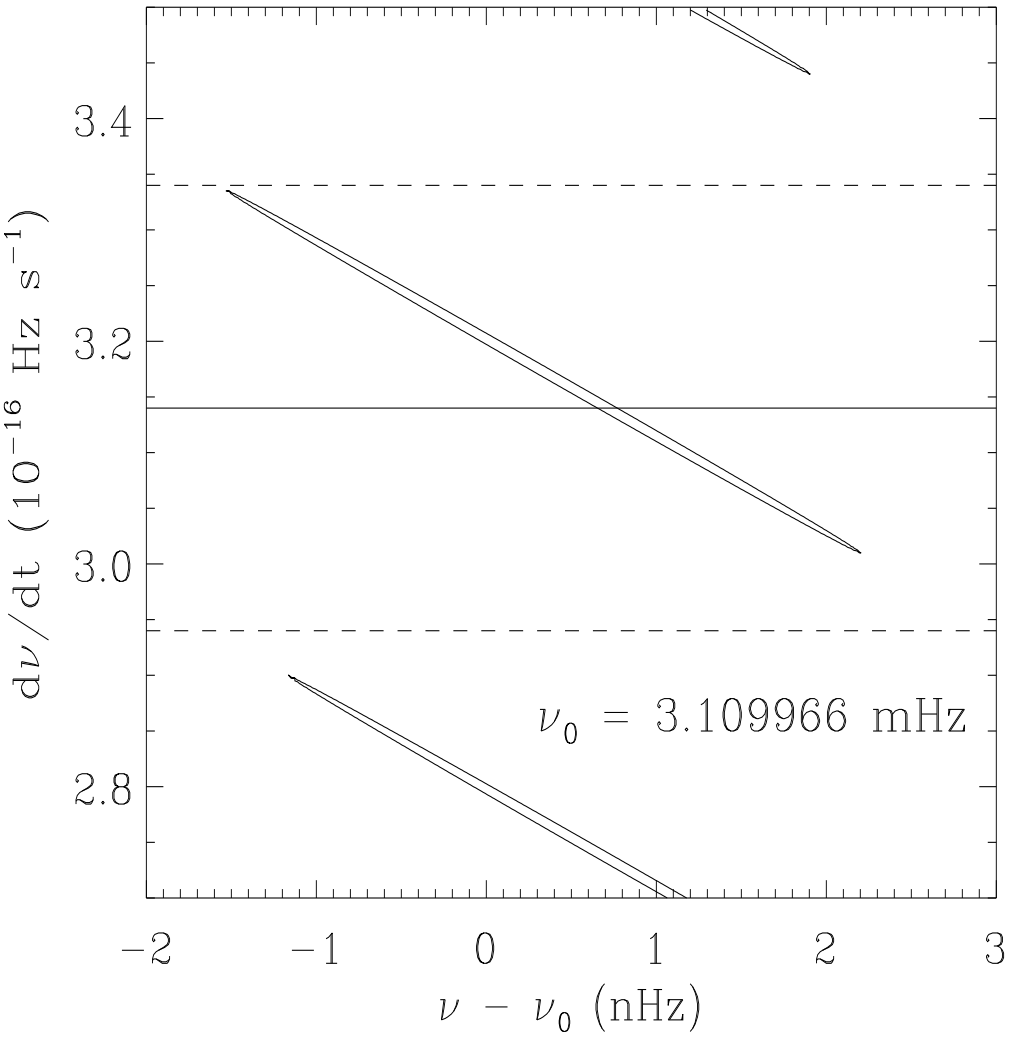

Figure 1a: Results of our ROSAT – Chandra timing study for J0806. (a) The 1σ confidence contours in the ν, $\dot{\nu}$ plane are shown in the vicinity of the lower $\dot{\nu} \approx 3 \times 10^{-16}$ Hz s^{-1} solution of Hakala et al. (2003). The best χ^2 for this solution was $\chi^2_{min} = 40.8$. The Hakala et al. solution and 1σ errors are marked by the horizontal solid and dashed lines, respectively. The nearby, "alias" solutions result from the sparseness of the ROSAT and Chandra observations. (b) Same as for Figure 1a, but in the vicinity of the $\dot{\nu} = 6 \times 10^{-16}$ Hz s^{-1} solution of Hakala et al. (2003). This solution has a better fit with $\chi^2_{min} = 33.1$.

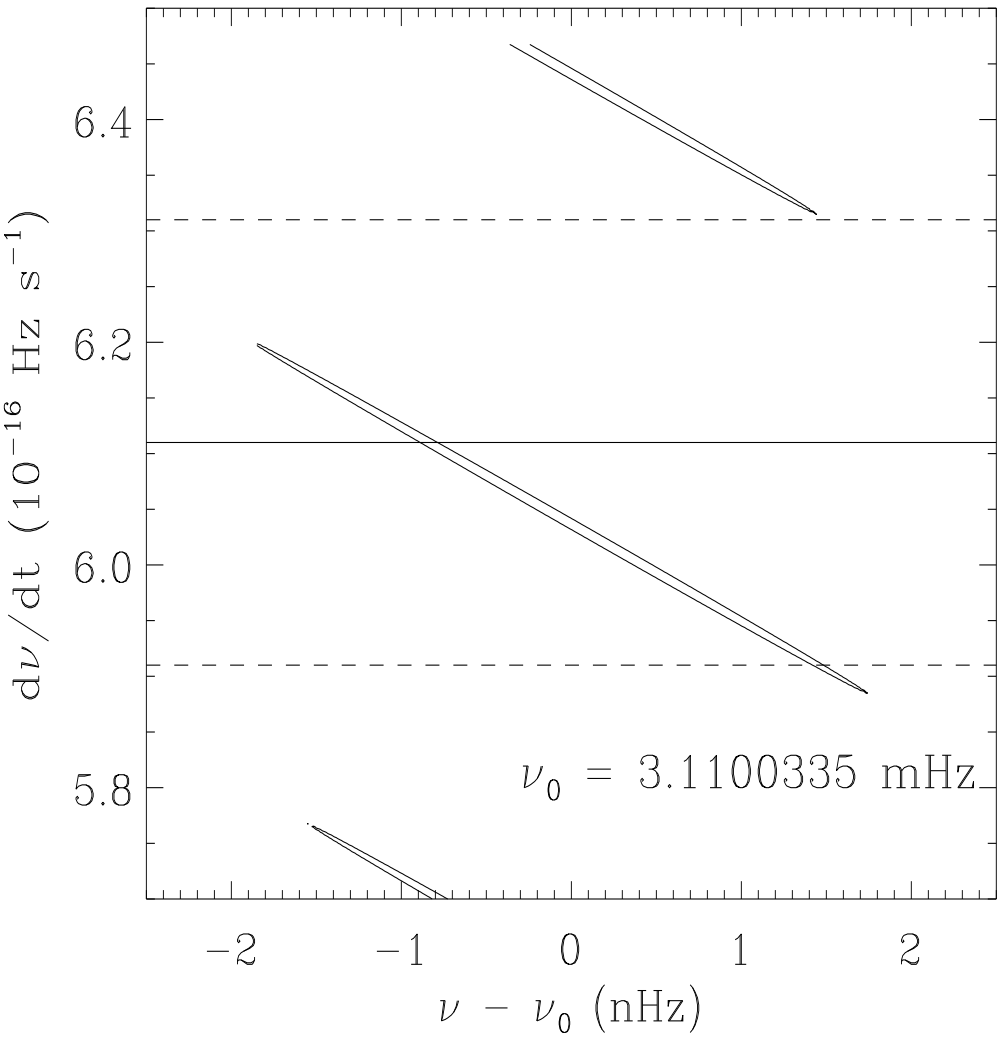

Figure 1b:

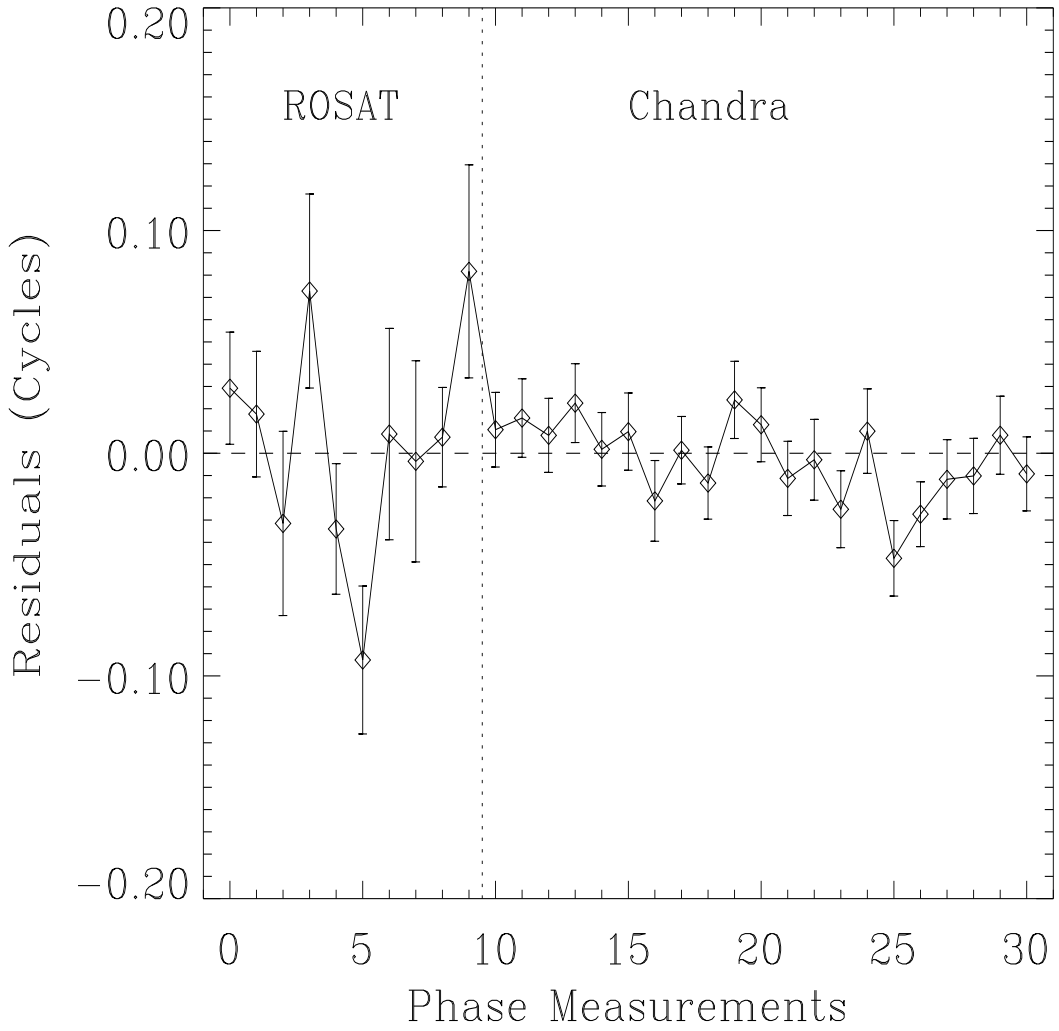

Figure 2a: Phase residuals from our ROSAT – Chandra timing study for J0806. (a) The phase residuals from the best fit consistent with the $\dot{\nu} \approx 3 \times 10^{-16}$ Hz s^{-1} solution of Hakala et al. (2003) are shown. The individual phase measurements are on the x-axis, and the vertical dotted line denotes the ROSAT and Chandra epochs. The long time gaps are essentially removed in this representation. (b) Same as Figure 2a, but for the $\dot{\nu} \approx 6 \times 10^{-16}$ Hz s^{-1} solution of Hakala et al. (2003). This solution has the better overall χ^2. Most of the improvement comes from the better fit to the ROSAT phases.

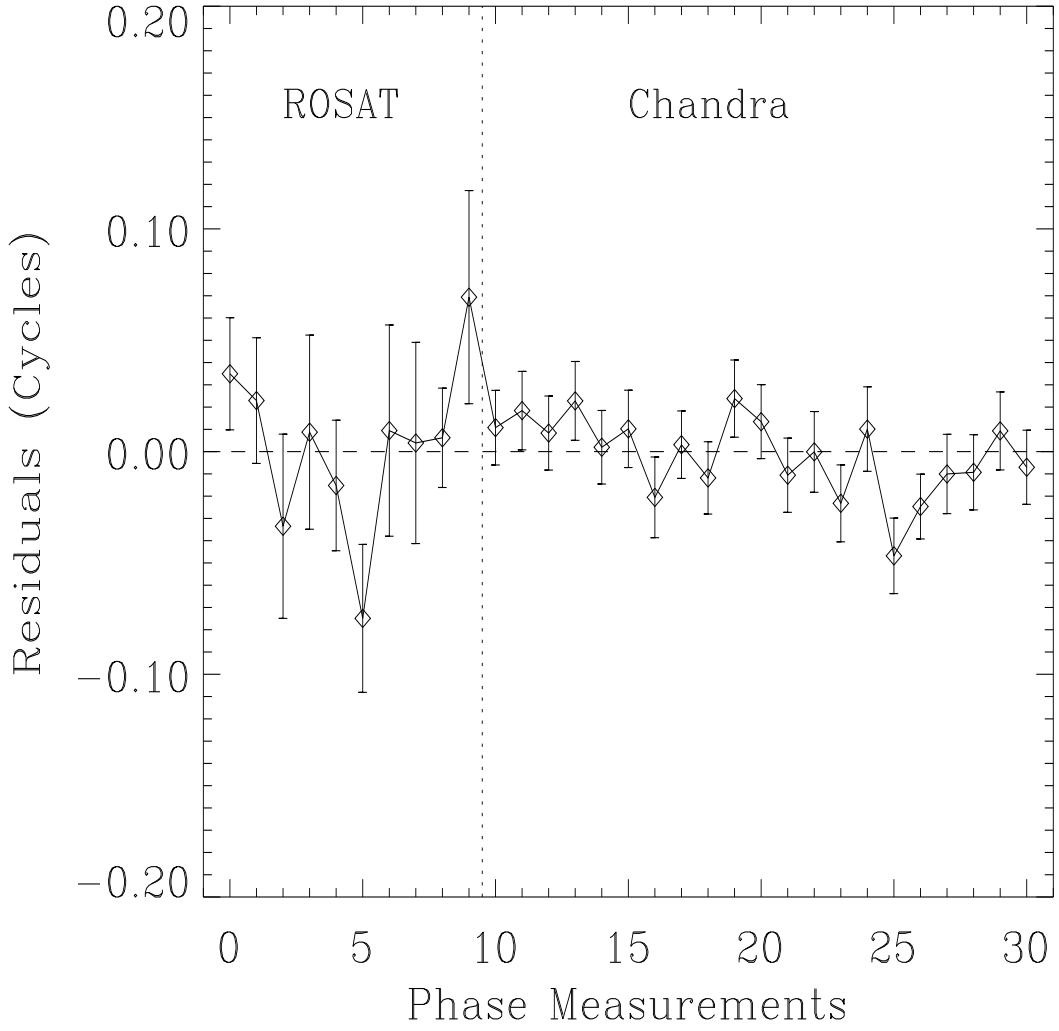
0.20
0.10
0.00
−0.10
−0.20
ROSAT
Chandra
Residuals (Cycles)
0
5
10
15
20
25
30
Phase Measurements

Figure 2b:

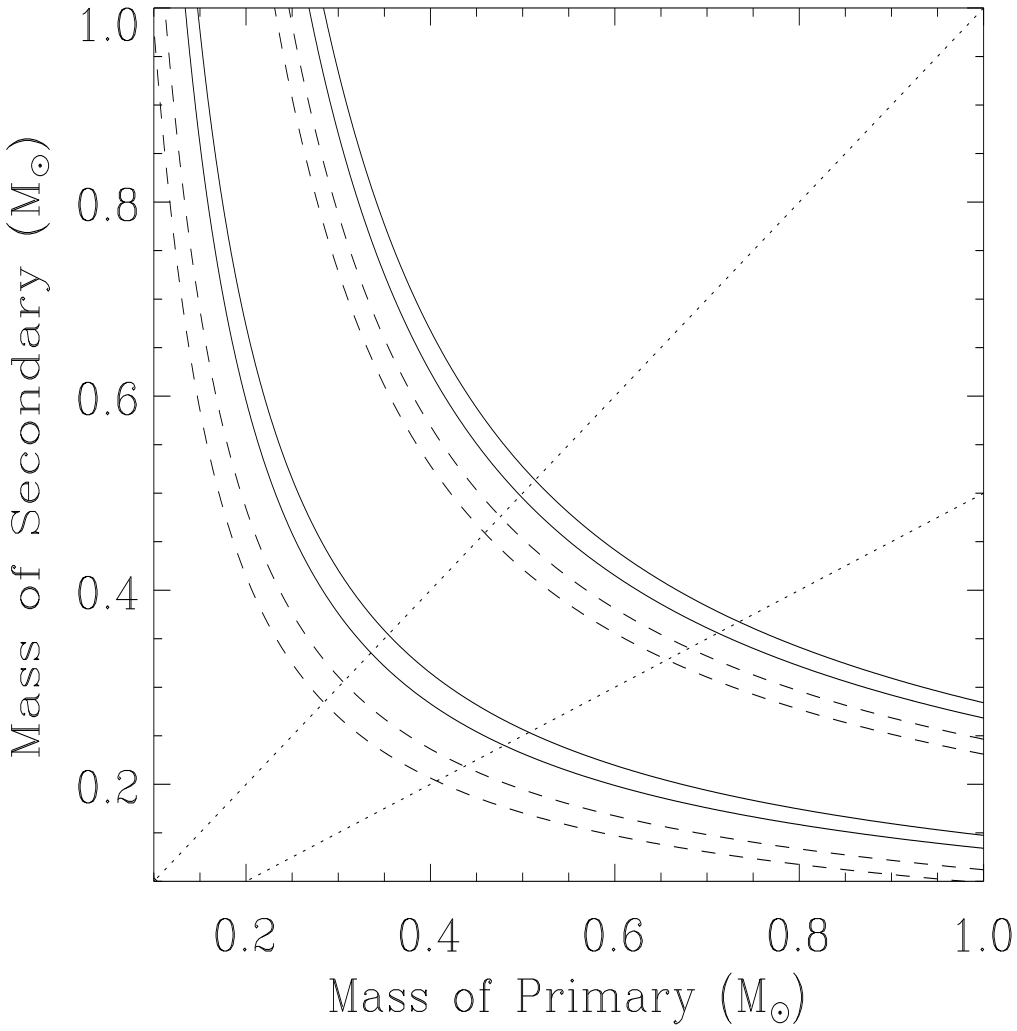

Figure 3: Constraints on the component masses of J0806 assuming that the orbital decay results only from gravitational radiation losses. The 1σ constraints for the 6×10^{-16} Hz s^{-1} (upper) and 3×10^{-16} Hz s^{-1} (lower) solutions are shown. In each case the solid and dashed curves are derived assuming no spin - orbit coupling, and full synchronization, respectively. The region between the dotted lines marks the phase space for which $0.5 < q = m_{sec}/m_{prim} < 1.0$.